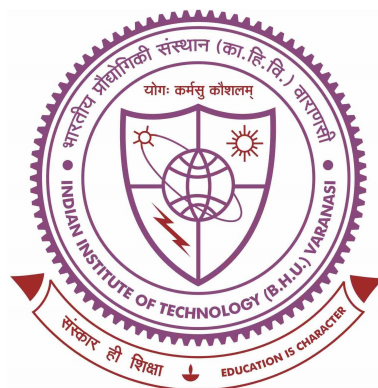


*ESTIMATION OF THE ENERGY BARRIER FOR MICELLE-MEDIATED
NUCLEATION GROWTH ON SURFACES: STRATEGIC REDUCTION
AND APPLICATION IN DRUG DELIVERY*



**Thesis submitted in partial fulfilment
for the Award of Degree**

Doctor of Philosophy

by

MONA VISHWAKARMA

DEPARTMENT OF CHEMICAL ENGINEERING & TECHNOLOGY

**INDIAN INSTITUTE OF TECHNOLOGY
(BANARAS HINDU UNIVERSITY)**

VARANASI – 221 005

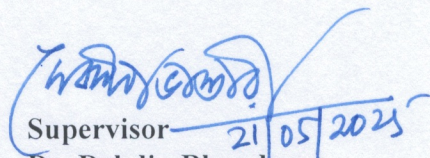
19041014

2025

CERTIFICATE

It is certified that the work contained in the thesis titled “*ESTIMATION OF THE ENERGY BARRIER FOR MICELLE-MEDIATED NUCLEATION GROWTH ON SURFACES: STRATEGIC REDUCTION AND APPLICATION IN DRUG DELIVERY*” by Ms. *MONA VISHWAKARMA* has been carried out under my supervision and that this work has not been submitted elsewhere for a degree.

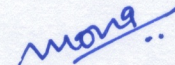
It is further certified that the student has fulfilled all the requirements of Comprehensive, Candidacy and SOTA.


Supervisor — 21/05/2025
Dr. Debdip Bhandary
Department of Chemical Engineering & Technology
Indian Institute of Technology
(Banaras Hindu University)
Varanasi – 221 005

DECLARATION BY THE CANDIDATE

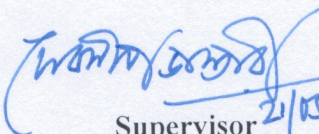
I, *MONA VISHWAKARMA*, certify that the work embodied in this thesis is my own bona fide work and carried out by me under the supervision of *DR. DEBDIP BHANDARY* from July 2019 to Jan 2025, at the *DEPARTMENT OF CHEMICAL ENGINEERING & TECHNOLOGY, Indian Institute of Technology (Banaras Hindu University) Varanasi*. The matter embodied in this thesis has not been submitted for the award of any other degree/diploma. I declare that I have faithfully acknowledged and given credits to the research workers wherever their works have been cited in my work in this thesis. I further declare that I have not willfully copied any other's work, paragraphs, text, data, results, *etc.*, reported in journals, books, magazines, reports, dissertations, theses, *etc.*, or available at websites and have not included them in this thesis and have not cited as my own work.

Date: May 21, 2025
Place: Varanasi, India

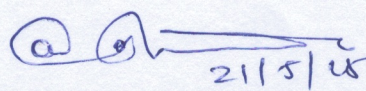

MONA VISHWAKARMA

CERTIFICATE BY THE SUPERVISOR

It is certified that the above statement made by the student is correct to the best of my knowledge.


Supervisor 21/05/2025

Dr. Debdip Bhandary
Assistant Professor
Dept. of Chemical Engg. & Tech.
IIT (BHU), Varanasi


21/5/25

Head of the Department
विभागाध्यक्ष / Head
रासायनिक अभियांत्रिकी एवं प्रौद्योगिकी विभाग
Deptt. of Chemical Engg. & Tech.
भारतीय प्रौद्योगिकी संस्थान / Indian Institute of Technology
काशी हिन्दू विश्वविद्यालय / Banaras Hindu University
वाराणसी / Varanasi-221005

COPYRIGHT TRANSFER CERTIFICATE


Title of the Thesis: Estimation of the Energy Barrier for Micelle-mediated Nucleation Growth on Surfaces: Strategic Reduction and Application in Drug Delivery

Name of the Student: Mona Vishwakarma

COPYRIGHT TRANSFER

The undersigned hereby assigns to the Indian Institute of Technology (Banaras Hindu University) Varanasi all rights under copyright that may exist in and for the above thesis submitted for the award of the Doctor of Philosophy.

Date: May 21, 2025
Place: Varanasi, India


MONA VISHWAKARMA

Note: However, the author may reproduce or authorize others to reproduce material extracted verbatim from the thesis or derivative of the thesis for author's personal use provided that the source and the Institute's copyright notice are indicated.

ABSTRACT

Poly elemental nanoparticles (PENPs) offer multi-functionality with exceptional properties such as high mechanical strength, thermal stability, and fatigue resistance, but their synthesis is energy-intensive and challenging. A solution-based approach using micelles (CTABs) mediated nucleation and growth is investigated to address this. The free energy of gold nucleation to be grown on a gold surface within a spherical micelle is estimated using the Umbrella Sampling method. An energy barrier of 10.36 ± 0.3 kcal/mol inhibited the nucleate-engulfed micelles from delivering the nucleate to the surface. Structural analysis showed that the spreading of micelle is essential to the discharge of engulfed nucleate. Adding a co-surfactant, oleylamine (OLA), with the primary surfactant, CTAB, formed a stable cylindrical micelle in water, which could reduce the energy barrier for the abovementioned purpose. The energy barrier decreases to 8.42 ± 0.3 kcal/mol in this case. Micelle deformation, influenced by OLA, facilitates nucleate release onto the surface, followed by an energy increase due to nucleate-surface interactions. However, a significant energy barrier persists despite these improvements, mainly due to hydration layers and micelle reorganization requirements. Reducing this energy barrier is crucial for optimizing nucleation and growth processes. The strong affinity between alkyl thiols and gold atoms was utilized to engineer the micelle's behaviour further. Hexadecane thiol molecules were infused into the micelle, and a subsequent reduction in the energy barrier was obtained (2.83 ± 0.12 kcal/mol). To make the process spontaneous, the energy barrier, due to strong water layering, has to be removed. A sparingly dispersed monolayer of thiols was introduced on the targeted surface. The decrease in the potential of mean force (PMF) and negative free energy changes demonstrated that thiol-functionalized surfaces can make the process spontaneous. The surface density of thiols was further varied to

optimize the energy barrier, and found that 3.34×10^{-6} mol/m² was the optimum density. Finally, we extended our study to the reverse drug release process from chitosan-based matrices. Encapsulating methotrexate (MTX) in a chitosan-stabilized system revealed an energy barrier of 81.1 ± 0.81 kcal/mol for release, which reduced to 52.4 ± 1.83 kcal/mol upon adding ethanol as a co-solvent. Further, it decreased to 5.33 ± 1.77 kcal/mol after replacing cross-linker STPP with Chloride ions. This highlighted the significant impact of solvent composition and cross-linkers like STPP on drug encapsulation and release.

ACKNOWLEDGEMENT

I would like to express my deepest gratitude to my thesis supervisor, Dr. Debdip Bhandary, for his invaluable guidance, encouragement, and continuous support throughout the course of my doctoral research. His mentorship not only introduced me to the field of molecular modelling and simulation methods but also inspired me to pursue research with curiosity and critical thinking.

I would like to sincerely acknowledge Prof. Monoj Kumar Mondal, Head, Department of Chemical Engineering and Technology, for his consistent support and for fostering a research-conducive environment that greatly facilitated the completion of this work. I am also deeply grateful to the Indian Institute of Technology (BHU) Varanasi for providing the infrastructure, academic environment, and resources that enabled the successful completion of this work. I am equally thankful to Dr. Abir Ghosh, Dr. Udit Uday Ghosh, and Dr. Pradip Paik for their suggestions and encouragement during research progress evaluation meetings, which helped me in improving various aspects of the journey.

I gratefully acknowledge the National Supercomputing Mission (NSM) for providing the computational resources of the PARAM Shivay Supercomputing Centre at the Indian Institute of Technology (BHU) Varanasi, which were essential for carrying out the simulations involved in this thesis. I am also thankful to the Ministry of Human Resource Development (MHRD), Government of India, for the financial support extended during my Ph.D. tenure at IIT (BHU) Varanasi.

I extend my sincere thanks to all the members of the **Soft & Condensed Matter Process Engineering Lab (SCoPE Lab)** and the Interfacial Science and Engineering Group for their collaboration and contributions to a stimulating research environment. In particular,

I wish to thank my labmates — Akanksha, Prateek, Chirag, Deepanshu, Priyanka, Mahesh, and Shweta — for their consistent support, discussions, and friendship. A special note of thanks goes to Dr. Sushma Yadav for her encouragement and insightful suggestions. I am equally grateful to my friends — Kanika, Abhishek, Vibhanshu, Kanhaiya, and Shakti— whose constant encouragement and unwavering support have made this journey more manageable and fulfilling.

A special note of appreciation goes to my brothers, Vikki and Vivek, whose unwavering support and encouragement helped me navigate the challenges of my Ph.D., particularly during the difficult times of the COVID-19 pandemic when the institute was closed. Their constant motivation and involvement, especially during critical phases of my work, have been truly invaluable.

Lastly, but most importantly, I am profoundly grateful to my parents and family for their unconditional love and steadfast support. Their belief in me has been my greatest strength throughout all phases of this journey. No words can truly capture the depth of my gratitude to them.

Best regards,

Mona Vishwakarma

Contents

Title	i
Certificate	iii
Candidate Declaration	v
Supervisor’s Certificate	v
Copyright Transfer Certificate	vii
Abstract	ix
Acknowledgement	xi
Table of Contents	xiii
List of Figures	xvii
List of Tables	xxvii
1 Introduction	1
1.1 Self Assembly	4
1.2 Surfactants	4
1.3 Micellization	6
1.3.1 Energetic Contributions to Micelle Formation	7
1.3.2 Generalized Free Energy Approach	9
1.4 Self-Assembled Monolayer	10
1.5 Nucleation	10
1.5.1 Nucleation Mechanism	12
1.6 Theories of Nucleation and Growth	12
1.6.1 LaMer- Brust nucleation	13
1.6.2 Finke-Watzky two-step nucleation mechanism	14
1.6.3 Coalescence and Orientation Attachment mechanism	14

1.7	Literature Review	15
1.8	Research Gap	21
1.9	Objectives	23
1.10	Nature and Scope of Present Work	23
2	Models and Methodology	27
2.1	Classical Molecular Dynamics	28
2.2	Molecular Modeling	30
2.3	Thermodynamic Ensembles	34
2.3.1	Microcanonical Ensemble	35
2.3.2	Canonical Ensemble	35
2.3.3	Grand-Canonical Ensemble	36
2.4	Property Calculation	36
2.4.1	Density Profile	36
2.4.2	Radial Distribution Function	37
2.4.3	Radius of Gyration	37
2.4.4	Potential of Mean Force	38
2.4.5	Steered Molecular Dynamics	39
2.4.6	Umbrella Sampling	39
2.4.7	Order Parameter	41
3	Estimation of Energy Barrier	43
3.1	Introduction	43
3.2	Methodology	46
3.3	Results and Discussion	49
3.4	Summary	59
4	Role of co-surfactant	61
4.1	Introduction	61
4.2	Models and Methodology	66
4.3	Results and Discussion	70

4.4	Summary	79
5	Role of co-surfactant thiols	81
5.1	Introduction	81
5.2	Model & Methodology	84
5.3	Results and Discussion	87
5.4	Summary	95
6	Role of Thiolated Layer	97
6.1	Introduction	97
6.2	Models and Methodology	99
6.3	Result and Discussion	101
6.4	Summary	109
7	A Drug Delivery Application	111
7.1	Introduction	111
7.2	Models and Methodology	115
7.3	Result and Discussion	117
7.4	Summary	129
8	Conclusions and Future Scopes	131
8.1	Conclusions	131
8.2	Future Scope	133
	List of Publications	135
	Bibliography	136

List of Figures

1.1	Schematic illustration of the structure of Poly-elemental nanoparticles (a) Metallic glasses, (b) High-Entropy alloys, (c) Intermetallic Compounds, (d) Multiphase Poly Elemental Nanoparticles, (e) Core-Shell. (Image is taken from ref[1])	1
1.2	(a) Schematic representation of Surfactant Molecule (b) Micellization Process. Colour code: blue circles- hydrophilic heads, black curved lines- hydrophobic tails.	6
1.3	Self-assembly of surfactants/amphiphiles on (a) hydrophobic surface forming hemimicelles. (b) and (c) a hydrophilic surface forming lamellar and cylindrical bilayers. Colour code: blue circles-hydrophilic heads, black curved lines-hydrophobic tails.	11
1.4	Typical diagram of self-assembled monolayer (SAM) formed by amphiphilic molecules on a substrate.	11
1.5	(a) Applications of SAMs.(Image is taken from ref[32])	12
1.6	(a) LaMer- Burst Nucleation Mechanism, (b) Growth Mechanism (Image is taken from ref[48])	13
1.7	Finke-Watzky two-step nucleation Mechanism (Image is taken from ref[49])	14
1.8	(a) Coalescence of platinum crystallites (b) Formation of titanium crystallites through orientated attachment (Image is taken from ref[50])	15
2.1	Schematic illustration of Lennard-Jones potential	31
2.2	Schematic illustration of Morse Potential	32
2.3	Schematic representation of (a) Periodic Boundary Condition, (b) Minimum Image convention	34

2.4	Radial distribution functions at different phases. Colour code: blue - solid, black - liquid, and grey - gas.	38
2.5	Umbrella Sampling (a) Pulling Simulation, (b) Simulation Window, (c) Histogram. (Image is taken from GROMACS Tutorial[112])	40
2.6	The tilt angle of self-assembled molecules on a solid surface.	41
3.1	(a) CTAB molecule, the nitrogen atom and bromide ion are represented as blue and purple spheres, respectively, and all the methyl groups are represented as cyan spheres. (b) Snapshot of the system containing a micelle of CTAB molecules in an aqueous media. Water has shown an ice-blue colour in continuous media. The blue rectangle represents the periodic box.	46
3.2	(a) Mass density profiles of different segments as a function of distance from the centre of mass of a CTAB micelle at 303 K (b) Radial distribution functions between the oxygen of water and N of the head group at different temperatures (c) Variation of Radius of gyration of the cationic part of micelle with temperature.	49
3.3	Snapshot of the system to show the attachment of CTAB micelles on a gold surface. The Au(111) surface, at the bottom, is represented in yellow spheres. Water molecules have shown an ice-blue colour. The blue rectangle represents the periodic box (not to scale in z-direction)	51
3.4	(a) Mass density of $(\text{CH}_3)_3\text{N}^+(\text{CH}_2)_-$, $-\text{CH}_3$, and H_2O as a function of distance from the gold surface (b) In-plane pair correlations for water molecules, ammonium groups and bromide ions.	52
3.5	Potential of mean force with distance ‘ d ’, which is the distance between the centre of mass of the gold nucleate and the top of the surface.	53
3.6	(a) Formation of Gold nucleates inside the micelle in solution.	55
3.7	Potential of mean force with a distance between the centre of mass of gold nucleate and the top of the gold (111) surface.	56

3.8	(a) Top view, (b) Side view, (c) Order parameter and variation of Radius of gyration with the distance between the center of mass of nucleate and gold (111) surface.	58
4.1	Molecular representation of the molecules – (a) CTAB and (b) Oleyamine – indicating their hydrophilic head and hydrophobic tail groups.	69
4.2	(a) Mass density profiles of different segments within the micelle – alkyl chains of CTAB and OLA, ammonium groups, amine groups, bromide ions, and water as a function of distance from the longitudinal axis of the cylindrical micelle at 303.15 K	71
4.3	(a) Formation of Gold nucleates inside the micelle in solution. (b) Formation of the number of nucleates as a function of time; Insets (I-III) contain the snapshots of nucleate formation at 0, 25 and 45 ns. (c) The radius of gyration of micelle with time. (d) The change in order parameter of OLA molecules in the y-direction (left axis) and CTAB molecules in the z-direction (right axis). Colour codes for molecular presentation are the same as in Figure 4.1; water is omitted for visual clarity. (e,f) Comparison of RDFs between the head group of surfactant molecules (red: CTAB and black: OLA) and water molecules after engulfing nucleates (solid lines) and that of a pure micelle (dashed line), respectively.	73
4.4	(a) Snapshot of the nucleate engulfed cylindrical micelle of CATB-OLA surfactants away from the gold surface in an aqueous media. The Au(111) surface, at the bottom, is represented in yellow spheres. Water has shown an ice-blue colour in continuous media. The blue rectangle represents the periodic box (not to scale in the z-direction). (b) Mass density of water and micelle as a function of distance from Au(111) gold surface. (c) In-plane pair correlations between water molecules in the layer adjacent to the Au(111) gold surface.	75

- 4.5 Potential of mean force between the centre of mass of gold nucleate and the top of the gold (111) surface. Snapshots inside the plot show the relative positions of nucleate and micelle on the surface. The black arrows indicate the position of the nucleate from the apex of the gold surface. The colour codes for molecular presentation are the same as in Figure 4.1, and water is omitted for clarity. 77
- 4.6 The top view and side view of a micelle containing nucleate are shown in (a) and (b), respectively. The colour codes for molecular presentation are the same as in Figure 4.1; the gold surface and water molecules are omitted for clarity. (c) The change in order parameter (right axis) and radius of gyration (left axis) of the micelle with distance between the centre of mass of gold nucleate and the top of the gold (111) surface. 79
- 5.1 Molecular representation of the molecules – (a) CTAB, (b) Oleyamine and (c) Hexadecanethiol – indicating their hydrophilic head and hydrophobic tail groups. For CTAB, the methyl groups, nitrogen atoms and bromide ions are represented as cyan, blue and purple spheres, respectively, whereas for oleylamine, the methyl groups, nitrogen atoms and hydrogen atoms are represented as red, pink and orange spheres, and for hexadecanethiol, the methyl groups and thiol group are represented sky blue and green spheres 87
- 5.2 (a) Mass density profiles of different segments; alkyl chain of CTAB, OLA and thiol, ammonium group, amine group, thiol group, bromide ions, and water as a function of distance from the centre of mass of a CTAB micelle at 303 K. The density profile of the ammonium group of CTAB, the amine group of co-surfactant OLA and the thiol group of co-surfactant HT are plotted on the right-side y-axis and rest on the left-side y-axis. 89

5.3	(a) Formation of Gold nucleates inside the micelle in an aqueous solution. (b) Formation of the number of nucleates as a function of time, Insets (I-VI) contain the snapshots of nucleate formation at 0, 1, 2, 15, 25, and 35 ns.	90
5.4	(a) Snapshot of the system containing a cylindrical micelle of co-surfactant OLA and thiol with CTAB molecules away from the gold surface in an aqueous media. The Au(111) surface, at the bottom, is represented in yellow spheres. Water has shown an ice-blue color continuous media. The blue rectangle represents the periodic box (not to scale in the z-direction). (c) Mass density of water and micelle as a function of distance from Au(111) gold surface.(c) In-plane pair correlations (radial distribution function) between water molecules in the layer adjacent to the Au(111) gold surface.	92
5.5	Potential of mean force between the centre of mass of gold nucleate and the top of the gold (111) surface. Snapshots inside the plot show the relative positions of nucleate and micelle on the surface. The black arrows indicate the nucleate's position from the apex of the gold surface. The color codes for molecular presentation are the same as in Figure 5.1, and water is omitted for visual clarity.	93
5.6	The top view and side view of a micelle containing nucleate are shown in (a) and (b), respectively. The color codes for molecular presentation are the same as in Figure 5.1; the gold surface and water molecules are omitted for clarity. (c)The radius of gyration (left axis) and change in order parameter (right axis) of the micelle with distance between the centre of mass of the gold nucleus and the top of the gold (111) surface.	94

- 6.1 a, b – Dispersed hexadecane thiol monolayer on a gold (111) surface – top and side view, respectively. The thiol groups are represented as green spheres, respectively, and all the methyl groups are represented in green. c,d – Cross-sectional (xz-plane) and longitudinal (along y-axis) view, respectively, of the cylindrical micelle formed by CTAB and OLA. For CTAB molecules, the nitrogen atoms and bromide ions are represented as blue and purple spheres, respectively, and all the methyl groups are represented as cyan-colored bonds. For OLA molecules, the nitrogen atoms and hydrogen atoms are represented as pink and orange spheres, respectively, and all the methyl groups are represented as red-colored bonds. Water has shown an ice-blue colour in continuous media. The blue rectangle represents the periodic simulation box. 102
- 6.2 (a) Snapshot of the system containing a cylindrical micelle of co-surfactant OLA with CTAB molecules on the thiol-functionalized gold surface in an aqueous media. The Au(111) surface, at the bottom, is represented in yellow spheres. Water has shown an ice-blue color continuous media. The blue rectangle represents the periodic box (not to scale in the z-direction). (b) Density profile of water, micelle and thiol molecules along the z-axis . 103
- 6.3 Potential of Mean Force (PMF) as a function of the distance (d) between the gold nucleate and the functionalized gold surface with hexadecane thiol molecules. Insets depict the structural configurations of the micelle containing gold nucleate at various stages along the reaction coordinate. The black arrows indicate the position of the nucleate from the apex of the thiolated layer on the gold surface. The color codes for molecular presentation are the same as in Figure 6.1, and water is omitted for visual clarity. 104
- 6.4 In-plane pair correlations (radial distribution function) between thiol molecules on Au(111) surface. Blue to red color gradient represents the RDF profiles at different surface densities of thiol molecules. 106

6.5	Potential of Mean Force (PMF) as a function of the distance (d) between the centre of mass of the gold nucleate and the thiol-functionalized gold surface for various surface densities of thiol molecules. Blue to red color gradient represents the PMF profiles at different surface densities of thiol molecules.	107
6.6	Change in free energy (ΔG) as a function of the surface density of thiol molecules (ρ_S)	108
7.1	Chemical structure of (a) Chitosan, (b) STPP, and (c) Methotrexate molecule. Blue and Red circles indicated the hydrogen bond donor and acceptor sites respectively.	117
7.2	(a) Snapshot of the system at the end of production run (50 ns); the blue box represents the simulation box filled with water; the CS - STPP were presented as a greenish bonded structure, and the MTX molecules were shown in red and brown bonded spheres. Water molecules were omitted here for clarity. (b) The density profiles of CS, STPP, MTX, and water were shown in respective colors against the reduced length of the simulation box.	118
7.3	The radial distribution for (a) CS-CS and CS-STPP pairs, (b) different components of the solutions with water (i.e. CS-WATER, STPP-WATER, and MTX-WATER). A dashed purple line is used to represent the RDF for the MTX-WATER pair in an aqueous solution. In Figures c and d, isosurface representations of the solvation shell of the MTX drug and CS monomer, respectively. Molecules are shown using bonded structures, and Oxygen atoms of water molecules are shown using red spheres.	119
7.4	Free energy landscape of the release of MTX into the water. The x-axis indicates the reaction coordinate in the reduced unit. The Cyan and green zones represent water and a CS-STPP matrix, respectively. Insets a and b show the snapshot of the binding of MTX with the CS-STPP matrix and an MTX molecule in water.	120

- 7.5 (a) Snapshot of the system at the end of the production run (50 ns). The simulation box filled with water is represented by the blue line; the MTX molecules were displayed as red and brown bonded spheres, and the CS - STPP were presented as a greenish bonded structure. The molecules of ethanol were shown as being pink in color. The colors of the Na⁺ and Cl⁻ ions were displayed as blue and light green, respectively. For clarity, water molecules were omitted here. (b) The density profiles of CS, STPP, MTX, ETHANOL, NaCl and water were shown with respective colors along the reduced length of the simulation box. 121
- 7.6 (a) The radial distribution function for CS-CS and CS-STPP in water and aqueous ethanol solution. Solid and dashed lines are used for the RDF in water and aqueous ethanol solution, respectively. (b) The radial distribution function between ethanol molecules and CS, STPP, and MTX pairs at 303 K is represented by black, red, and purple lines, respectively. A dashed purple line indicates the radial distribution of ethanol molecules around MTX molecules in an aqueous solution of ethanol. 123
- 7.7 Free energy landscape of the release of MTX into the ethanol-water solution. The x-axis indicates the reaction coordinate in nm. The Cyan and green zones represent water and a CS-STPP matrix, respectively. Insets a and b show the snapshot of the binding of MTX with the CS-STPP matrix and an MTX molecule in an ethanol-water solution. 124
- 7.8 (a) Snapshot of the system after the production run where CS was represented as the green bond structure, MTX molecules were shown in red and brown bonded spheres, and ethanol molecules were represented as pink bonds, Na⁺ and Cl⁻ ions are shown as blue and light green spheres, respectively. 125

-
- 7.9 Free energy landscape of the release of MTX into the ethanol-water solution in the absence of cross-linker STPP. The x-axis indicates the reaction coordinate in nm. The Cyan and green zones represent water and a CS matrix, respectively. Insets a and b show the snapshot of the binding of MTX with the CS matrix and an MTX molecule in an ethanol-water solution. 126
- 7.10 (a) Density profile of STPP along the reduced length of the simulation box, blue to red color gradient shown the density profile of STPP as TPP replaced with an equivalent number of chloride ions, (b) Radial distribution function of chloride ions – CS pairs as removal of TPP from 0 to 100 %, blue to red color gradient represents the RDF profiles of chloride ions – CS pairs at the different extent of chloride ions. 127
- 7.11 Change in free energy for the release of MTX molecules at different fractions of STPP, the cross-linker of CS, was replaced by NaCl. The inset shows the change in the CS-MTX pair correlation function in the presence (purple line) and absence (red line) of STPP in the solution. 128

List of Tables

3.1	Force Field Parameters for the CTAB and Water molecules.	48
4.1	Force Field Parameters for Oleylamine Molecules.	68
5.1	Force Field Parameters for Hexadecanethiol Molecules.	86
6.1	Lennard-Jones (LJ) and Morse Potential Parameters of United Atoms . . .	99

